arXiv:1410.1720v3 [physics.bio-ph] 24 Nov 2014

Enhanced active swimming in viscoelastic fluids

Emily E. Riley and Eric Lauga
Department of Applied Mathematics and Theoretical Physics, University of Cambridge, Cambridge CB3 0WA, United Kingdom.

Swimming microorganisms often self propel in fluids with complex rheology. While past theoretical work indicates that fluid viscoelasticity should hinder their locomotion, recent experiments on waving swimmers suggest a possible non-Newtonian enhancement of locomotion. We suggest a physical mechanism, based on fluid-structure interaction, leading to swimming in a viscoelastic fluid at a higher speed than in a Newtonian one. Using Taylor's two-dimensional swimming sheet model, we solve for the shape of an active swimmer as a balance between the external fluid stresses, the internal driving moments, and the passive elastic resistance. We show that this dynamic balance leads to a generic transition from hindered rigid swimming to enhanced flexible locomotion. The results are physically interpreted as due to a viscoelastic suction increasing the swimming amplitude in a non-Newtonian fluid and overcoming viscoelastic damping.

PACS numbers: 47.63.Gd, 47.63.-b, 47.50.-d

I. INTRODUCTION

Active locomotion allows many types of motile cells to adapt to their environment and ensure their survival [1]. One type of oft-studied locomotion is the flagella- or cilia-based swimming of microorganisms [2]. In many instances, their locomotion occurs through biological or environmental fluids containing proteins and other polymers which display elastic, and non-Newtonian, characteristics. Important examples include mucus transport by lung cilia [3], nematodes travelling though soil [4], bacteria in their host's tissue [5], and spermatozoa swimming though cervical mammalian mucus [6].

The majority of work on small-scale swimming has focused on swimmers self-propelling in Newtonian fluids. Recently, a few experimental and theoretical studies have addressed the role of non-Newtonian stresses in the fluid, with conflicting conclusions as to their impact on locomotion. On the one hand, measurements with Boger fluids show enhanced propulsion of a flapping flexible swimmer [7] and of a cylindrical swimming sheet [8]. While a rotating helix in a Boger fluid displayed decreased swimming at small amplitude, it underwent a modest enhancement at larger helical amplitudes [9]. In contrast, the locomotion of the nematode *C. elegans* was shown to be systematically hindered in a Boger fluid [10], and similarly locomotion in shear-thinning fluids showed a systematic decrease [8]. Additionally recent computational studies on *C. elegans* showed that both flexibility and back-front asymmetry in stresses are required for enhanced propulsion [11].

In parallel to experiments, analytic studies of locomotion using a prescribed, small-amplitude flagellar waveform predicted a systematic decrease in swimming speed in viscoelastic fluids [12–14]. Enhanced swimming has been predicted to occur as either due to end effects and stress singularities [15] or for large-amplitude swimming [9].

In this work we propose a dynamic mechanism for swimming enhancement in a viscoelastic fluid. Instead of prescribing the shape of the flagellar deformation we solve for the waveform of the swimmer as a balance between the fluid stresses and the internal driving and resisting forces, similarly to work on actuated finite-size filaments [13] and synthetic swimmers [16]. We then show that this dynamic balance leads to a generic transition from hindered rigid swimming to enhanced flexible locomotion.

II. WAVING MOTION IN VISCOELASTIC FLUIDS

In order to model active swimming, we consider Taylor's two-dimensional waving model [17], which is suitable for the physical description of beating eukaryotic flagella and cilia [2, 12]. The extension to the case of three-dimensional filaments is presented in the appendix, with similar results.

Consider an infinite, two-dimensional sheet of negligible thickness, as illustrated in fig. 1. It is embedded in a viscous fluid, and due to internal actuation is made to deform its shape as a traveling wave of frequency ω, amplitude a, wave number k, and wave speed $c = \omega/k$, and self-propels as a result with speed U in the opposite direction. At low Reynolds number, which is the relevant limit for microorganisms, the flow around the sheet is described by the incompressible Cauchy equations, $\nabla\cdot\boldsymbol{\tau} = \nabla p$, $\nabla\cdot\mathbf{u} = 0$, with p the pressure, $\mathbf{u}$ the velocity field, and $\boldsymbol{\tau}$ the deviatoric stress. We use a stream function ψ such that $u_x = \partial\psi/\partial y$ and $u_y = -\partial\psi/\partial x$, in order to enforce incompressibility.

Viscoelastic effects in the fluid are modelled using the classical Oldroyd-B evolution equation for $\boldsymbol{\tau}$. That model, which can be rigorously derived from a dilute solution of infinitely-extensible elastic dumbbells in a Newtonian solvent [18], captures many features of Boger (elastic, constant viscosity) fluids such as those used in experiments on propulsion [7, 8, 10, 19]. In the Oldroyd-B model, the deviatoric stress $\boldsymbol{\tau}$ is written as a sum,

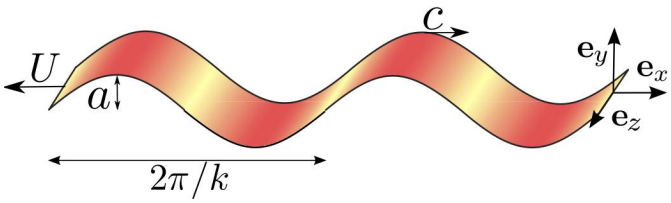

FIG. 1: A two-dimensional flexible sheet deforming as a traveling wave with amplitude a, wave number k, wave speed c, and frequency $\omega = kc$ resulting in its swimming at speed U.

$\boldsymbol{\tau} = \boldsymbol{\tau}_s + \boldsymbol{\tau}_p$, of a Newtonian solvent, $\boldsymbol{\tau}_s$, with viscosity η_s, and a polymeric stress, $\boldsymbol{\tau}_p$, satisfying a Maxwell model with relaxation time λ and viscosity η_p (and thus elastic modulus $G \equiv \eta_p/\lambda$). The total deviatoric stress, $\boldsymbol{\tau}$, satisfies the Oldroyd-B constitutive equation,

$$\boldsymbol{\tau} + \lambda \overset{\triangledown}{\boldsymbol{\tau}} = \eta\dot{\boldsymbol{\gamma}} + \eta_s\lambda \overset{\triangledown}{\dot{\boldsymbol{\gamma}}}, \tag{1}$$

where the total viscosity is $\eta = \eta_s + \eta_p$ and where $\dot{\boldsymbol{\gamma}}$ is the shear rate tensor, $\dot{\boldsymbol{\gamma}} = \nabla\mathbf{u} + \nabla\mathbf{u}^T$. In eq. (1), we used $\overset{\triangledown}{\mathbf{A}} = \partial\mathbf{A}/\partial t + \mathbf{u}\cdot\nabla\mathbf{A} - (\nabla\mathbf{u}^T\cdot\mathbf{A} + \mathbf{A}\cdot\nabla\mathbf{u})$, to denote the upper convected derivative for any tensor $\mathbf{A}$. An important factor in the derivations below will be $\beta = \eta_s/\eta < 1$, ratio of solvent to total viscosity. The relative importance of viscoelasticity is quantified by the Deborah number, $\mathrm{De} = \lambda\omega$, ratio of the relaxation time of the polymers to the relevant time-scale of the waving motion, ω^{-1}.

III. SWIMMING SPEED

Assuming that the waveform of the sheet is known, we first solve for the external fluid dynamics. The height of the sheet is written as $y(x,t) = \epsilon y_1(x,t) + \epsilon^2 y_2(x,t) + \ldots$, where $\epsilon \ll 1$ denotes the dimensionless waving amplitude. The leading-order shape, y_1, is decomposed as

$$y_1(x,t) = \mathrm{Re}\left[\sum_{n\geq 1} a^{(n)} e^{in(kx-\omega t)}\right], \tag{2}$$

where Re denotes the real part, and $a^{(n)}$ is the amplitude of the nth Fourier mode. Using the Fourier notation $W = \mathrm{Re}\left[\sum_{n\geq 1}\tilde{W}^{(n)}e^{-in\omega t}\right]$ to describe the nth mode $\tilde{W}^{(n)}$ of a time-periodic function W, we thus have $\tilde{y}_1^{(n)} = a^{(n)}e^{inkx}$.

Denoting by $a_{\mathrm{NN}}^{(n)}$ the sheet amplitude in a non-Newtonian (Oldroyd-B) fluid and by $a_{\mathrm{N}}^{(n)}$ the Newtonian one, we can solve for the external fluid dynamics asymptotically in powers of ϵ following the work in refs. [12, 20]. Swimming is obtained at order ϵ^2, at dimensional speeds in the non-Newtonian (NN) case given by

$$U_{\mathrm{NN}} = \tfrac{1}{2}\sum_{n=1}^{\infty} n^2\omega k|a_{\mathrm{NN}}^{(n)}|^2\left(\frac{1+\beta n^2\mathrm{De}^2}{1+n^2\mathrm{De}^2}\right), \tag{3}$$

while in the Newtonian (N) limit we obtain

$$U_{\mathrm{N}} = \tfrac{1}{2}\sum_{n=1}^{\infty} n^2\omega k|a_{\mathrm{N}}^{(n)}|^2. \tag{4}$$

If the swimmer has identical shape in both fluids, *i.e.* $a_{\mathrm{NN}}^{(n)} = a_{\mathrm{N}}^{(n)}$, comparing eqs. (3) and (4) shows that we always have $U_{\mathrm{NN}} < U_{\mathrm{N}}$ since $\beta < 1$. In order to obtain an enhancement of the swimming speed in a viscoelastic fluid, a physical mechanism must thus exist to increase $|a_{\mathrm{NN}}^{(n)}|$ beyond $|a_{\mathrm{N}}^{(n)}|$. As we show below, solving for the swimmer amplitude by enforcing the correct dynamic balance allows us to obtain a nontrivial dependence of $a_{\mathrm{NN}}^{(n)}$ on the Deborah number, and enhancement. As both eqs. (3) and (4) are quadratic in the amplitudes $a^{(n)}$, we note that we only need derive the first order shape dynamics.

IV. DYNAMIC BALANCE OF ACTIVE SWIMMER

Within a beating eukaryotic flagellum there are three forces to consider. Firstly, the internal driving due to the spatio-temporal actuation from molecular motors [21]. We model this internal forcing, classically, as due to a time-varying distribution of active bending moments per unit length, $F(x,t)$ [22]. Balancing this actuation are two resisting forces, the external hydrodynamics stresses (pressure and viscous stresses) and the internal solid mechanics resistance (elastic cost to be bent away from a preferred, flat state) [23]. Note that any potential internal dissipation is neglected compared to dissipation in the outside fluid. Denoting the bending stiffness of the sheet κ, normal force balance at leading order in the amplitude of the sheet deformation is written as

$$-\kappa\nabla^4 y + \hat{\mathbf{n}}\cdot\boldsymbol{\sigma}\cdot\hat{\mathbf{n}}|_S = \nabla^2 F, \tag{5}$$

where $\hat{\mathbf{n}}$ is the unit normal to the sheet at leading order and $\boldsymbol{\sigma}$ the hydrodynamic stress tensor.

In order to determine the hydrodynamic stress, we consider the constitutive equation, eq. (1), at leading order

$$\left(1+\lambda\frac{\partial}{\partial t}\right)\boldsymbol{\tau}_1 = \eta\left(1+\beta\lambda\frac{\partial}{\partial t}\right)\dot{\boldsymbol{\gamma}}_1, \tag{6}$$

where we have expanded each quantity in powers of $\epsilon \ll 1$, $\boldsymbol{\tau} = \epsilon\boldsymbol{\tau}_1 + \ldots$; $\dot{\boldsymbol{\gamma}} = \epsilon\dot{\boldsymbol{\gamma}}_1 + \ldots$, etc. Writing eq. (6) using Fourier notation we have

$$\tilde{\boldsymbol{\tau}}_1^{(n)} = \frac{\eta - in\lambda\omega\eta_s}{1-in\lambda\omega}\tilde{\dot{\boldsymbol{\gamma}}}_1^{(n)} = \frac{1-in\mathrm{De}\beta}{1-in\mathrm{De}}\eta\tilde{\dot{\boldsymbol{\gamma}}}_1^{(n)}. \tag{7}$$

The first order Stokes equation similarly reduces to

$$\eta\nabla\cdot\tilde{\dot{\boldsymbol{\gamma}}}_1^{(n)} = \frac{1-in\mathrm{De}}{1-in\mathrm{De}\beta}\nabla\tilde{p}_1^{(n)}, \tag{8}$$

at leading order in ϵ. The pressure is eliminated from the above by taking its curl, leaving the biharmonic equation for the stream function, $\nabla^4\tilde{\psi}_1^{(n)} = 0$. This is solved in Fourier space to obtain the first order stream function as

$$\psi_1 = \mathrm{Re}\left[\sum_{n=1}^{\infty}\frac{\omega}{k}a_{\mathrm{NN}}^{(n)}(1+nky)e^{-nky}e^{in(kx-\omega t)}\right]. \quad (9)$$

Notably, the flow described by eq. (9) is the same as the Newtonian solution, hence viscoelasticity does not modify the flow induced by the swimmer at leading order. However, as we see below, it does impact the stress distribution. In order to determine the pressure, we have to integrate eq. (8) using eq. (9) leading to

$$\tilde{p}_1^{(n)} = -2\eta\omega k\left(\frac{1-in\mathrm{De}\beta}{1-in\mathrm{De}}\right)in^2a_{\mathrm{NN}}^{(n)}e^{-nky}e^{inkx}. \quad (10)$$

The hydrodynamic stress tensor, $\boldsymbol{\sigma}$, is given by $\boldsymbol{\sigma} = -p\mathbf{I}+\boldsymbol{\tau}$, which, at leading order, reduces in Fourier space to

$$\tilde{\boldsymbol{\sigma}}_1^{(n)} = -\tilde{p}_1^{(n)}\mathbf{I} + \frac{1-in\mathrm{De}\beta}{1-in\mathrm{De}}\eta\tilde{\dot{\gamma}}_1^{(n)}, \quad (11)$$

for each Fourier mode n.

With the determination of the fluid stress, eq. (5) can be written in Fourier components as

$$-\kappa\frac{\partial^4\tilde{y}_1^{(n)}}{\partial x^4} - \frac{\partial^2\tilde{F}_1^{(n)}}{\partial x^2} = \tilde{p}_1^{(n)} + 2\eta\left(\frac{1-in\mathrm{De}\beta}{1-in\mathrm{De}}\right)\frac{\partial^2\tilde{\psi}_1^{(n)}}{\partial y\partial x}\bigg|_S \quad (12)$$

Writing $F_1 = \mathrm{Re}\left[\sum_{n\geq 1}f^{(n)}e^{in(kx-\omega t)}\right]$ to describe the first order contribution to the active bending moment, we can determine the leading-order dynamic response of the sheet amplitude and obtain

$$a_{\mathrm{NN}}^{(n)} = \frac{-k^2f^{(n)}}{-\kappa n^2k^4 + 2\eta\omega ik\left(\frac{1-in\mathrm{De}\beta}{1-in\mathrm{De}}\right)}. \quad (13)$$

As can be seen in eq. (13), the value of the Deborah number impacts the sheet amplitude, and thus the swimmer waveform is modified by a change in the surrounding fluid.

Inputting the linear waveform amplitude, eq. (13), into the quadratic swimming speed, eq. (3), we finally obtain the non-Newtonian swimming speed as

$$U_{\mathrm{NN}} = \frac{\omega}{2k}\sum_{n=1}^{\infty}\left[\frac{n^2|f^{(n)}|^2}{\kappa^2k^2}\left(\frac{1+n^2\beta\mathrm{De}^2}{1+n^2\mathrm{De}^2}\right)\times \frac{1}{n^4+4\mathrm{Sp}^6\left(\frac{1+n^2\beta^2\mathrm{De}^2}{1+n^2\mathrm{De}^2}\right)+4n^3\mathrm{Sp}^3\left(\frac{\mathrm{De}(1-\beta)}{1+n^2\mathrm{De}^2}\right)}\right], \quad (14)$$

where we have defined the (two-dimensional) Sperm number, $\mathrm{Sp} = (\eta\omega/\kappa k^3)^{1/3}$, which quantifies the dimensionless ratio of fluid to bending stresses [24]. If $\mathrm{Sp} \ll 1$, the dominant balance is between activity and elasticity, and the flagellum waveform is not affected by fluid stresses – this is the stiff (s) limit. In contrast, when $\mathrm{Sp} \gg 1$, fluid effects balance the active bending and the waveform changes with the properties of the fluid – this is the floppy (f) limit.

Simplifying the analysis to focus on the single $n = 1$ mode (reducing notation to $f^{(n)} \equiv f$), we have non-Newtonian swimming at speed

$$U_{\mathrm{NN}} = \frac{|f|^2}{2\kappa^2k^2}\frac{\omega}{k}\times \frac{\left(1+\beta\mathrm{De}^2\right)}{1+\mathrm{De}^2+4\mathrm{Sp}^6\left(1+\beta^2\mathrm{De}^2\right)+4\mathrm{Sp}^3\left[\mathrm{De}(1-\beta)\right]}, \quad (15)$$

while the Newtonian limit is found by setting $\mathrm{De} = 0$ in eq. (15). The non-Newtonian to Newtonian swimming speed ratio, $R = U_{\mathrm{NN}}/U_{\mathrm{N}}$, is thus given by

$$R = \frac{(1+4\mathrm{Sp}^6)(1+\beta\mathrm{De}^2)}{1+\mathrm{De}^2+4\mathrm{Sp}^3\mathrm{De}(1-\beta)+4\mathrm{Sp}^6(1+\beta^2\mathrm{De}^2)}, \quad (16)$$

which is the main result of this paper.

V. ENHANCED LOCOMOTION

In order to derive the conditions under which swimming enhancement is possible, we need to understand when the function $R(\beta, \mathrm{De}, \mathrm{Sp})$ can be above one. Let us first consider some relevant physical limits. In the stiff limit, $\mathrm{Sp} \ll 1$, eq. (16) simplifies to the fixed-amplitude result [12]

$$R = \frac{1+\beta\mathrm{De}^2}{1+\mathrm{De}^2}. \quad (17)$$

In that limit, the swimming speed ratio decreases monotonically with increasing Deborah number to the asymptotic value $U_{\mathrm{NN}} = (\eta_s/\eta)U_{\mathrm{N}}$ for $\mathrm{De} \gg 1$.

In the opposite floppy limit, $\mathrm{Sp} \gg 1$, the flagellum shape is highly sensitive to changes in the hydrodynamic stress and the speed ratio, eq. (16), reduces to

$$R = \frac{1+\beta\mathrm{De}^2}{1+\beta^2\mathrm{De}^2}. \quad (18)$$

Here, we obtain a systematic monotonic increase of the swimming speed with Deborah numbers, up to an asymptotic value $R = 1/\beta$ obtained when $\mathrm{De} \gg 1$.

Our model points therefore to a transition from hindered to enhanced swimming when the flagellum is sufficiently flexible. To get further insight, let us look at small deviations from the Newtonian limit ($\mathrm{De} = 0$). Computing the derivate of R with respect to De we get $\partial R/\partial\mathrm{De}|_{\mathrm{De}=0} = 4(\beta-1)\mathrm{Sp}^3/(1+4\mathrm{Sp}^6)$, which is always

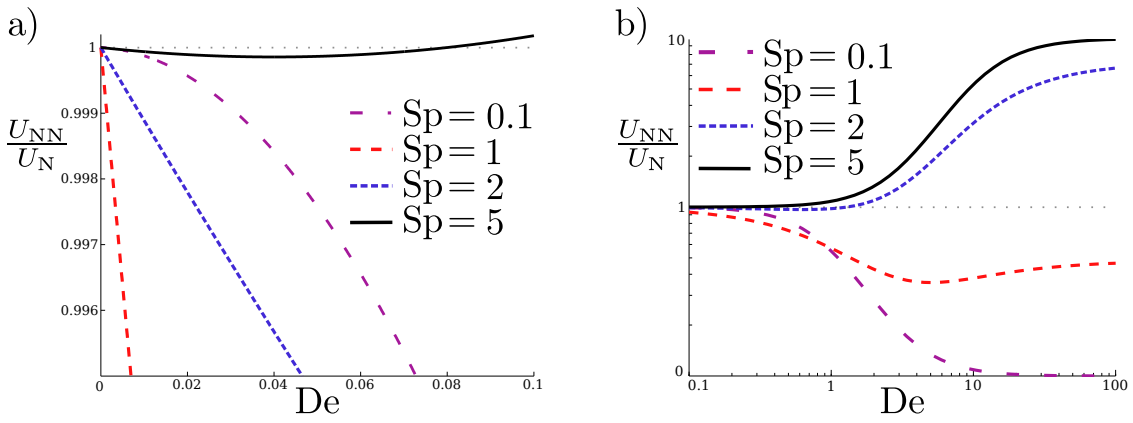

FIG. 2: Ratio of non-Newtonian to Newtonian swimming speed, U_{NN}/U_N, as a function of the Deborah number, De, for four different values of the Sperm numbers ($\beta = 0.1$ corresponding to a critical value of Sp $\gtrsim 1.16$ for enhanced swimming, eq. (20)).

negative. Consequently, a small amount of viscoelasticity (De $\ll 1$) will always start by decreasing the swimming speed. In contrast, in the infinite Deborah number limit, the swimming speed ratio becomes

$$R(\mathrm{De} \gg 1) = \frac{\beta + 4\beta \mathrm{Sp}^6}{1 + 4\beta^2 \mathrm{Sp}^6}. \tag{19}$$

A transition from hindered ($R < 1$) to enhanced propulsion ($R > 1$) in a non-Newtonian fluid occurs thus when

$$\mathrm{Sp}^3 > \frac{1}{2\sqrt{\beta}}. \tag{20}$$

The result in eq. (20) indicates therefore a transition in swimmer flexibility allowing enhancement of the swimming speed. Indeed, the Sperm number scales inversely proportional to the flagellum bending modulus, and thus for a given fluid, the criterion in eq. (20) is equivalent to a requirement for κ to be small enough.

Our results are illustrated numerically in fig. 2 for $\beta = 0.1$. We plot the ratio of the non-Newtonian to Newtonian swimmer speed, U_{NN}/U_N, as a function of the Deborah number for four different values of the Sperm number. The data are shown in fig. 2a for small values of De and ranging from 0 to 100 in fig. 2b. In all cases, the swimming speed initially decreases with the Deborah number (fig. 2a) but when the swimmer is sufficiently flexible, the swimming speed subsequently increases and crosses the threshold $U_{NN}/U_N = 1$ (fig. 2b). The criterion from eq. (20) corresponds to enhancement predicted to occur as soon as Sp $\gtrsim 1.16$, consistent with the numerical results. Note that our model also allows us to compute the value of the transition Deborah number beyond which enhancement occurs. In eq. (16), one can solve the quadratic equation for De and $R > 1$ is equivalent to De $> 4\mathrm{Sp}^3/(4\beta\mathrm{Sp}^6 - 1)$, which, as expected, is defined only if the criterion in eq. (20) is satisfied.

Beyond swimming kinematics, our model also allows us to compute swimming energetics and efficiency. Following ref. [12] and the derivations above, we can calculate the power expanded by the swimmer against the fluid, $\dot{\mathcal{W}}_{NN}$. Defining the swimming efficiency, classically, as $\mathcal{E} = \eta U^2/\dot{\mathcal{W}}$, the ratio between the non-Newtonian efficiency and that in a Newtonian fluid with the same viscosity (η) is exactly given by the swimming speed ratio R from Eq. (16). The conditions for enhanced swimming correspond thus to those required for enhanced efficiency.

VI. ILLUSTRATION OF THE WAVEFORM

We further illustrate the impact of non-Newtonian stresses by displaying the swimming waveform in the case of an internal sinusoidal forcing. We thus prescribe $f^{(1)} = fi$ and $f^{(n)} = 0$ for $n > 1$, and compute the leading-order waveform. Under the assumption of linear response, the shape remains sinusoidal with a different phase and amplitude. The results are illustrated in fig. 3 for three Sperm numbers (1, 2 and 10) and four Deborah numbers (0, 1, 2, and ∞). Superimposed on the shapes are the values of R, ratio of the non-Newtonian to Newtonian swimming speeds.

The results in fig. 3 show the expected decrease in waving amplitude that accompanies an increase in Sperm number but, more importantly, the systematic increase in amplitude with an increase of viscoelasticity De. The waving amplitudes can be computed analytically and we obtain the Newtonian result as $A_N^2 = 1/(1 + 4\mathrm{Sp}^6)$, which explains the decrease of waving amplitude with Sperm number. In the non-Newtonian case we have a waving amplitude given by

$$A_{NN}^2 = \frac{1 + \mathrm{De}^2}{1 + \mathrm{De}^2 + 4\mathrm{Sp}^3\mathrm{De}(1-\beta) + 4\mathrm{Sp}^6(1 + \beta^2\mathrm{De}^2)}. \tag{21}$$

The critical Deborah number for which $A_{NN} > A_N$ is then found to be De $> 1/\mathrm{Sp}^3(1+\beta)$, which is always satisfied. Hence the presence of viscoelastic stresses leads to a systematic increase of the waving amplitude of the

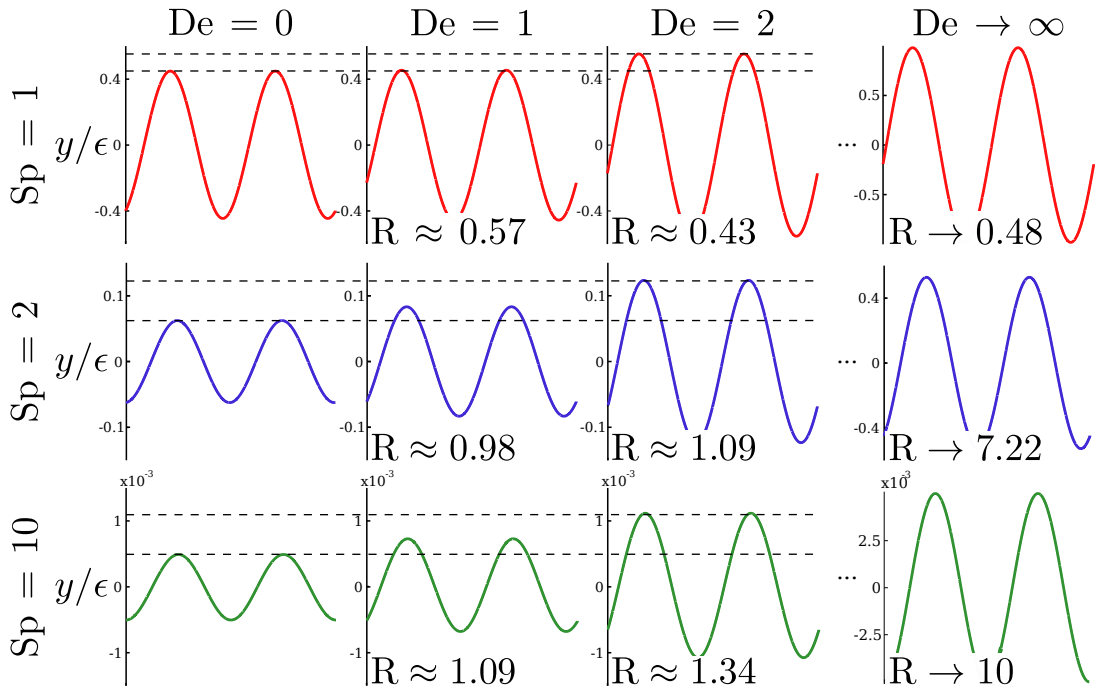

FIG. 3: Swimming waveforms under a linear response for Sp = 1, 2, and 10, as a function of the Deborah number, De. In each plot, the value of the swimming ratio, $R = U_{\mathrm{NN}}/U_{\mathrm{N}}$, is indicated. As in fig. 2 $\beta = 0.1$ and Sp $\gtrsim 1.16$ is required for enhancement. An increase in De leads to an increase in waving amplitude which, when sufficiently large, leads to enhanced swimming.

swimmer. This provides a physical interpretation for the swimming enhancement seen in fig. 2: if the viscoelastic amplitude increase is large enough, it is able to compensate for the non-Newtonian damping term from eq. (3), leading to faster swimming, $U_{\mathrm{NN}} > U_{\mathrm{N}}$.

VII. DISCUSSION

In this paper, we have proposed a physical mechanism for enhanced locomotion in a viscoelastic fluid. It does not require transient or end effects but instead arises naturally due to the equations of active elastohydrodynamics applied to locomotion.

Our results can be rationalised by focusing on the two different stiff (s) and floppy (f) limits, and comparing the non-Newtonian swimming speed for De $\gg 1$ to the Newtonian one (De $= 0$). In the stiff regime fluid forces are negligible, and the dynamic balance in eq. (12) reduces to one between bending resistance and active stresses. Considering only the typical magnitudes of a and f, we then get $a^{(s)} \sim f/\kappa k^2$ for both Newtonian and non-Newtonian. The swimming speeds scale then as $U_{\mathrm{N}}^{(s)} \sim \omega f^2/\kappa^2 k^3$ and, for large De, $U_{\mathrm{NN}}^{(s)} \sim \beta\omega f^2/\kappa^2 k^3$, leading to $R^{(s)} = \beta < 1$. In contrast, in the floppy regime, elastic forces are negligible compared to fluid stresses, and the dynamic balance in eq. (12) reduces to one between the fluid resistance of the filament and the active stresses, with $a_{\mathrm{N}}^{(f)} \sim kf/\eta\omega$ and $a_{\mathrm{NN}}^{(f)} \sim kf/\eta\omega\beta$. The swimming speeds in this case are given by $U_{\mathrm{N}}^{(f)} \sim k^3 f^2/\eta^2\omega$ and $U_{\mathrm{NN}}^{(f)} \sim k^3 f^2/\beta\eta^2\omega$, leading to $R^{(f)} = 1/\beta > 1$, and enhanced swimming.

Physically, we have shown that the transition from hindered to enhanced swimming takes its origin in the systematic increase of the waving amplitude for active swimming in a viscoelastic fluid, which can overcome viscoelastic fluid damping [12]. How can this increase in amplitude be intuitively rationalised? We would like to argue that it is a consequence of the change in fluid pressure, and results from a 'viscoelastic suction'. Indeed, we consider the leading-order pressure in eq. (10), and compute its typical value on the sheet for a fixed amplitude a, allowing us to isolate the change in pressure due to the fluid dynamics and not due to the amplitude increase. The ratio between the typical non-Newtonian and Newtonian pressure is then

$$\left[\frac{p_{\mathrm{NN}}(a)}{p_{\mathrm{N}}(a)}\right]^2 = \frac{1+\beta^2\mathrm{De}^2}{1+\mathrm{De}^2}, \tag{22}$$

which shows a large pressure reduction (since $\beta < 1$) in a viscoelastic fluid. For sufficiently large Sperm numbers, where fluid stresses have a relatively larger impact on the waveform, the wave amplitude increase due to this suction effect is able to overcome the non-Newtonian fluid damping in locomotion and increase the swimming speed.

To conclude, we note that although the mechanism outlined in this paper was derived in the context of flagellar locomotion, the same physical principle would be at

$\tilde{p}$	$-\eta\omega k\tilde{h}i\cos\theta AK_1(kr)$
$\tilde{u}_r$	$-\tilde{h}\omega i\cos\theta[\alpha ArkK_1(kr)+BK_2(kr)+CK_0(kr)]$
$\tilde{u}_\theta$	$-\tilde{h}\omega i\sin\theta[BK_2(kr)-CK_0(kr)]$
$\tilde{u}_x$	$-\tilde{h}\omega\cos\theta[\alpha ArkK_0(kr)+(B+C-\alpha A)K_1(kr)]$
αA	$\left\{K_0(kb)+bkK_1(kb)\left[\frac{1}{2}+\frac{K_0(kb)}{2K_2(kb)}-\frac{K_0(kb)^2}{K_1(kb)^2}\right]\right\}^{-1}$
B	$-\alpha AbkK_1(kb)/[2K_2(kb)]$
C	$[1-bkK_1(kb)\alpha A/2]/K_0(kb)$

TABLE I: Pressure and velocity field for a travelling wave in the $\mathbf{e}_x$ direction on a cylinder to first-order in $\ln(kb)$, with $\alpha=(1-i\mathrm{De})/(1-i\beta\mathrm{De})$ [14].

play for higher swimmers exploiting muscular contractions, and thus could also be relevant to the dynamics of small multicellular organisms in complex environments.

Appendix: infinite filament

Having studied a two-dimensional waving sheet, we outline how to carry out the calculation a three-dimensional infinite filament, following ref. [25]. Consider an infinite periodic filament in an Oldroyd-B fluid waving with small amplitude. The filament is modelled geometrically as a cylinder, which when straight is parametrised by s along its axis, ϕ around this axis, and radius b. When small-amplitude waves propagate along $\mathbf{e}_x$, the surface of the cylinder is described by $\hat{\mathbf{r}}=[h(s,t)+b\cos\phi]\mathbf{e}_y+b\sin\phi\mathbf{e}_z+s\mathbf{e}_x$ and the height of the filament away from its centreline position is

$$h(s,t)=\epsilon\mathrm{Re}\left[a_{\mathrm{NN}}e^{i(ks-\omega t)}\right], \tag{A.1}$$

where a is the amplitude, and $h(s,t)$ is analogous to $y(x,t)$ in the above when $n=1$. Using the first-order Oldroyd-B equation, in Fourier notation, we recover eq. (7). We can then consider the Stokes equation at first order,

$$\nabla^2\tilde{\mathbf{u}}_1=\eta\left(\frac{1-i\beta\mathrm{De}}{1-i\mathrm{De}}\right)\nabla\tilde{p}_1, \tag{A.2}$$

where the first order boundary conditions for each mode are given by $\tilde{\mathbf{u}}_1=i\omega\tilde{h}\mathbf{e}_y$. The solutions are best derived using cylindrical polar co-ordinates, where the basis vectors are $\mathbf{e}_x$, $\hat{\mathbf{r}}=\sin\phi\mathbf{e}_z+\cos\phi\mathbf{e}_y$ and $\hat{\theta}=-\sin\phi\mathbf{e}_y+\cos\phi\mathbf{e}_z$. The first-order solutions are shown in table I [14]. These can then be used to compute the second-order swimming speed, leading to the same result as eq. (3). The force per unit length acting of the fluid is found by integrating the stress around the circumference and keeping only lowest-order terms in $\ln(kb)$ the force per unit length perpendicular to the filament is

$$\mathcal{F}_{vis}=\mathrm{Re}\left[-i\omega a_{\mathrm{NN}}\frac{4\pi}{\ln(kb)}\frac{1-i\beta\mathrm{De}}{1-i\mathrm{De}}\eta e^{i(ks-\omega t)}\right]. \tag{A.3}$$

This viscoelastic force is then balanced by the passive elastic forces of the filament and the internal forcing,

$$\tilde{\mathcal{F}}_{vis}=-2b\frac{\partial^2\tilde{F}_1}{\partial s^2}-\kappa\frac{\partial^4\tilde{h}}{\partial s^4}\,, \tag{A.4}$$

where F_1 is the first-order bending moment per unit length, as above. The non-Newtonian swimming velocity is then finally given by

$$U_{\mathrm{NN}}=\frac{2b^2\left|f\right|^2}{\kappa^2k^2}\frac{\omega}{k}\times\frac{\left(1+\beta\mathrm{De}^2\right)}{1+\mathrm{De}^2+2\mathrm{Sp}^4\mathrm{De}(1-\beta)+\mathrm{Sp}^8\left(1+\beta^2\mathrm{De}^2\right)}, \tag{A.5}$$

where we have defined the perpendicular drag coefficient $\xi_\perp=4\pi\eta/\ln(kb)$, and the three-dimensional Sperm number, $\mathrm{Sp}=(\xi_\perp\omega/\kappa k^4)^{1/4}$. The three dimensional result, eq. (15), is thus very similar to the two-dimensional case, and the physical mechanism identified in this paper extends naturally to three dimensions.

Acknowledgments

We thank RE Goldstein and TJ Pedley for useful discussions. This work was funded in part by the European Union (CIG grant to EL).

[1] D. Bray *Cell Movements* Garland Publishing, New York 2000
[2] S. Childress *Mechanics of Swimming and Flying* Cambridge University Press, Cambridge 1981
[3] M. A. Sleigh, J. R. Blake and N. Liron *Am. Rev. Respir. Dis.* 137:726, 1988
[4] H. R. Wallace *Annu. Rev. Phytopathol.* 6:91, 1967
[5] C. Josenhans and S. Suerbaum *Int. J. Med. Microbiol.* 291:605, 2002
[6] S. S. Suarez and A. A. Pacey *Hum. Reprod. Update* 12:23, 2006
[7] J. Espinosa-Garcia, E. Lauga and R. Zenit *Phys. Fluids* 25:031701, 2013
[8] M. Dasgupta, B. Liu, H. C. Fu, M. Berhanu, K. S. Breuer, T. R. Powers and A. Kudrolli *Phys. Rev. E* 87:013015, 2013
[9] Spagnoli S. E., Lui B. and Powers T. R. *Phys. Rev. Lett.*1110681012013
[10] X. Shenand P. E. Arratia *Phys. Rev. Lett.* 106:208101, 2011
[11] B. Tomases and R. D. Guy *Phys. Rev. Lett.* 113:098102, 2014

[12] E. Lauga *Phys. Fluids* 19:083104, 2007
[13] H. C. Fu, T. R. Powers and C. W. Wolgemuth *Phys. Rev. Lett.* 99:258101, 2007
[14] H. C. Fu, C. W. Wolgemuth and T. R. Powers *Phys. Fluids* 21:033102, 2009
[15] J. Teran, L. Fauci and M. Shelley *Phys. Rev. Lett.* 104:038101, 2010
[16] M. P. Curtis and E. A. Gaffney *Phys. Rev. E* 87:043006, 2013
[17] G. I. Taylor *Proc. R. Soc. London Ser. A* 209:447, 1951
[18] N. Phan-Thein *Understanding Viscoelasticity: An Introduction to Rheology* Springer, Singapore 2012
[19] B. Lui, T. R. Powers and K. S. Breuer *PNAS* 108:19516, 2011
[20] G. J. Elfring *Symmetry Breaking and Synchronisation at Small Scales* PhD Thesis, UC San Diego 2012
[21] C. J. Brokaw *Science* 243:1593, 1989
[22] S. Camalet and F. Jülicher *New J. Phys.* 2:24, 2000
[23] A. A. Evans and E. Lauga *Phys. Rev. E* 84:031924, 2011
[24] C. H. Wiggins and R. E.Goldstein *Phys. Rev. Lett.* 80:3879, 1998
[25] H. C. Fu, C. W. Wolgemuth and T. R. Powers *Phys. Rev E* 78:041913, 2008